

Human Urine-derived Stem Cells Seeded Surface Modified Composite Scaffold Grafts for Bladder Reconstruction in a Rat Model

Jun Nyung Lee,^{1*} So Young Chun,^{2*}
Hyo-Jung Lee,² Yu-Jin Jang,³
Seock Hwan Choi,¹ Dae Hwan Kim,⁴
Se Heang Oh,⁵ Phil Hyun Song,⁶
Jin Ho Lee,⁷ Jong Kun Kim,⁸
and Tae Gyun Kwon¹

¹Department of Urology, Kyungpook National University School of Medicine, Daegu; ²Bio-Medical Research Institute, Kyungpook National University Hospital, Daegu; ³Department of Neural Development and Disease, Korea Brain Research Institute, Daegu; ⁴Department of Laboratory Animal Research Support Team, Yeungnam University, Daegu; ⁵Department of Nanobiomedical Science & WCU Research Center, Dankook University, Cheonan; ⁶Department of Urology, Yeungnam University College of Medicine, Daegu; ⁷Department of Advanced Materials, Hannam University, Daejeon; ⁸Department of Emergency Medicine, Kyungpook National University School of Medicine, Daegu, Korea

*Jun Nyung Lee and So Young Chun contributed equally to this work.

Received: 1 June 2015
Accepted: 2 September 2015

Address for Correspondence:

Tae Gyun Kwon, MD
Department of Urology, Kyungpook National University School of Medicine, 130 Dongdeok-ro, Jung-gu, Daegu 41944, Korea
Tel: +82.53-200-2671, Fax: +82.53-200-3029
E-mail: tgkwon@knu.ac.kr

Funding: This research was supported by Basic Science Research Program through the National Research Foundation of Korea (NRF) funded by the Ministry of Science, ICT & Future Planning (grant number) (2014R1A1A3049460); (NRF-2014M3A9D3033887); funded by the Ministry of Education (2015R1D1A3A03020378); and supported by a grant of the Korea Health Technology R&D Project through the Korea Health Industry Development Institute (KHIDI), funded by the Ministry of Health & Welfare (HI14C1642)

We conducted this study to investigate the synergistic effect of human urine-derived stem cells (USCs) and surface modified composite scaffold for bladder reconstruction in a rat model. The composite scaffold (Polycaprolactone/Pluronic F127/3 wt% bladder submucosa matrix) was fabricated using an immersion precipitation method, and heparin was immobilized on the surface via covalent conjugation. Basic fibroblast growth factor (bFGF) was loaded onto the heparin-immobilized scaffold by a simple dipping method. In maximal bladder capacity and compliance analysis at 8 weeks post operation, the USC-scaffold^{heparin-bFGF} group showed significant functional improvement (2.34 ± 0.25 mL and 55.09 ± 11.81 μ L/cm H₂O) compared to the other groups (2.60 ± 0.23 mL and 56.14 ± 9.00 μ L/cm H₂O for the control group, 1.46 ± 0.18 mL and 34.27 ± 4.42 μ L/cm H₂O for the partial cystectomy group, 1.76 ± 0.22 mL and 35.62 ± 6.69 μ L/cm H₂O for the scaffold group, and 1.92 ± 0.29 mL and 40.74 ± 7.88 μ L/cm H₂O for the scaffold^{heparin-bFGF} group, respectively). In histological and immunohistochemical analysis, the USC-scaffold^{heparin-bFGF} group showed pronounced, well-differentiated, and organized smooth muscle bundle formation, a multi-layered and pan-cytokeratin-positive urothelium, and high condensation of submucosal area. The USC-seeded scaffold^{heparin-bFGF} exhibits significantly increased bladder capacity, compliance, regeneration of smooth muscle tissue, multi-layered urothelium, and condensed submucosa layers at the in vivo study.

Keywords: Bladder Regeneration; Surface Modified Scaffold; Urine-derived Stem Cells; Basic Fibroblast Growth Factor 2

INTRODUCTION

Bladder augmentation remains one of the greatest surgical challenges in the field of urology. Conventional bladder reconstruction using gastrointestinal tissue is associated with a series of complications (mucus production, bacterial colonization, electrolyte imbalances, or malignancy), significant morbidity, and functional alterations (1). Tissue engineering technique can circumvent many of these limitations and therefore has become considered as a potential alternative for bladder reconstruction.

The chief obstacle over the years to reconstructing the bladder through regeneration has been the absence of an ideal biomaterial that can provide a structurally intact low-pressure reservoir, serve as a scaffold for the healing and regeneration of the bladder wall, and retain normal function until it is replaced by host tissues (2,3). Until recently, three classes of biomaterials have been extensively investigated for bladder tissue engineering. Naturally derived materials, e.g. collagen (4) and alginate (5), acellular tissue matrices, e.g., bladder submucosa (BSM) (6) and small intestinal submucosa (7), and synthetic polymers, e.g., polyglycolic acid (PGA) (8), polylactic acid (PLA) (9), and poly-lactic-co-glycolic acid (PLGA) (10). However, none of them could provide required results for ideal biomaterials. In an effort to fabricate a scaffold that can be applied to morphological and functional bladder reconstruction, we have been worked to develop a composite scaffold composed with synthetic and natural derived biomaterial. As a synthetic biomaterial, polycaprolactone (PCL) was investigated as a potential substi-

tute for bladder tissue reconstruction because of its flexibility, biocompatibility, stability, and resistance to resorption (11). We could fabricate a blend of PCL with Pluronic F127 (F127) and bladder submucosa matrix (BSM), which has been shown to be a non-immunogenic, non-cytotoxic collagen-rich membrane that can be rapidly replaced by native tissues (12).

In our previous work, the PCL/F127/3 wt% BSM composite scaffold exhibited significantly enhanced hydrophilicity, the surface was easily immobilized, and there was no evidence of teratoma formation in vivo (12). Based on our previous results, we fabricated an advanced scaffold containing a specific growth factor to enhance proliferation of smooth muscle cells and urothelial cells, which are the two essential cell types for functional bladder regeneration. Basic fibroblast growth factor (bFGF) has been shown to stimulate the proliferation and survival of both smooth muscle and urothelial cells (13), thus suggesting the benefits of bFGF-loaded scaffolds for urological tissue engineering applications. Therefore, to fabricate a scaffold for bFGF delivery, we covalently conjugated heparin to the surface of a scaffold to form a heparin-immobilized scaffold, which was then loaded with bFGF (scaffold^{heparin-bFGF}) (14).

Tissue engineering of bladder also requires ideal cell source. Autologous cells are one of the most popularly used cells with the advantages including, decreased infection, require no immunosuppression reagents, and do not require histocompatibility matching (15). However, autologous bladder cell harvest procedures are surgically invasive, and the prolonged cell expansion methods are expensive, subject to contamination, and unrealistic for routine clinical use. Alternative sources of healthy and abundant bladder tissue are desired for optimal bladder engineering and bladder regeneration. Skeletal muscle cells, bone marrow stromal cells, embryonic, and parthenogenetic stem cells are all currently under investigation as potential future alternatives, however these modalities are in their infancy. For the purpose of this study, we turned to a stem cell source from urine, i.e., urine-derived stem cells (USCs). USCs have been proposed as an alternative stem cell source for urological tissue reconstruction since they have mesenchymal stem cell characteristics and have demonstrated the capacity to differentiate into a variety of urological cell lineages (16).

In this study, we hypothesized that a USC-seeded scaffold-heparin-bFGF graft would promote regeneration of the bladder wall. To investigate the synergic effect of the USC-scaffold-heparin-bFGF in terms of smooth muscle and urothelial layer regeneration, the scaffold-heparin-bFGF was characterized by quantifying the amounts of immobilized heparin and loaded bFGF released, and assessing the biocompatibility and differentiation of USCs in vitro. In addition, the potential of the USC-scaffold-heparin-bFGF for bladder reconstruction was evaluated in vivo using a rat model.

MATERIALS AND METHODS

Fabrication of the heparin-immobilized bFGF-loaded scaffold (scaffold^{heparin-bFGF})

PCL (MW 80,000 Da; Sigma-Aldrich, St. Louis, MO, USA), tetraglycol (glycofuro; Sigma-Aldrich), Pluronic F127 (MW 12,500 Da; BASF, Ludwigshafen, Germany), and BSM were used for scaffold fabrication. BSM was prepared as described in our previous report, and the formulation consisting of 3 wt% BSM of the polymer base was chosen (12). The PCL/F127/BSM scaffold was prepared using an immersion precipitation method (17). A PCL pellet/Pluronic F127 powder mixture (95/5 [w/w]) was dissolved in tetraglycol (12 wt%), and BSM powder was evenly mixed with the polymer solution. The mixed solutions were poured into a polytetrafluoroethylene mold (70 × 70 × 0.4 μL) and then directly immersed in water for 1 hr at room temperature. After additional washing and vacuum drying, the PCL/F127/BSM composite scaffold was sterilized using ethanol.

Heparin (MW 18,000 Da; Sigma-Aldrich) was immobilized to the scaffold to bind bFGF to the scaffold. The scaffold was pre-wet with 70% (v/v) ethanol, washed with deionized water, and hydrated with a 0.1 M 2-(N-morpholino) ethanesulfonic acid (MES) buffer (pH 5.5). The carboxylic acid groups of heparin were activated using 1-ethyl-3-(3-dimethylaminopropyl) carbodiimide hydrochloride (EDC) and N-hydroxylsuccinimide (NHS) for 4 hrs. The scaffold was soaked in 10 mL of the heparin solution with gentle agitation at 48°C for 6 hr. The heparin-immobilized scaffold was rinsed with the 0.1 M MES buffer (pH 5.5) solution and phosphate buffered saline (PBS, pH 7.4) (18). The heparin-immobilized scaffold was soaked in PBS containing 100 ng/mL of bFGF (Peprotech, Rocky Hill, NJ, USA) and 1 mg/mL of bovine serum albumin (Sigma-Aldrich) for 4 hr with gentle agitation, and then the scaffold was washed with PBS (Fig. 1).

Determination of heparin and bFGF content

Heparin content on the scaffold surface was determined by the toluidine blue colorimetric method (19,20). The scaffold was placed in 1 mL of 0.2% NaCl solution, then 1 mL of toluidine blue solution was added, and inner air was removed. After 10 min of vibration, 2 mL of hexane was added and mixed by vortexing. The absorbance of the aqueous layers at 631 nm was determined by a UV spectrophotometer. Immobilized heparin was visualized by labeling with fluorescein isothiocyanate (FITC, 1 mg/mL) at 4°C for 3 hr. The FITC-labeled scaffold was cryosectioned (20 μm) and observed under a confocal laser-scanning microscope (LSM510, Carl Zeiss, Oberkochen, Germany).

For the bFGF affinity and release test, the scaffold^{heparin-bFGF} was immersed in 1 mL of PBS containing 1% bovine serum albumin at 37°C for 28 days. The solution was collected and re-

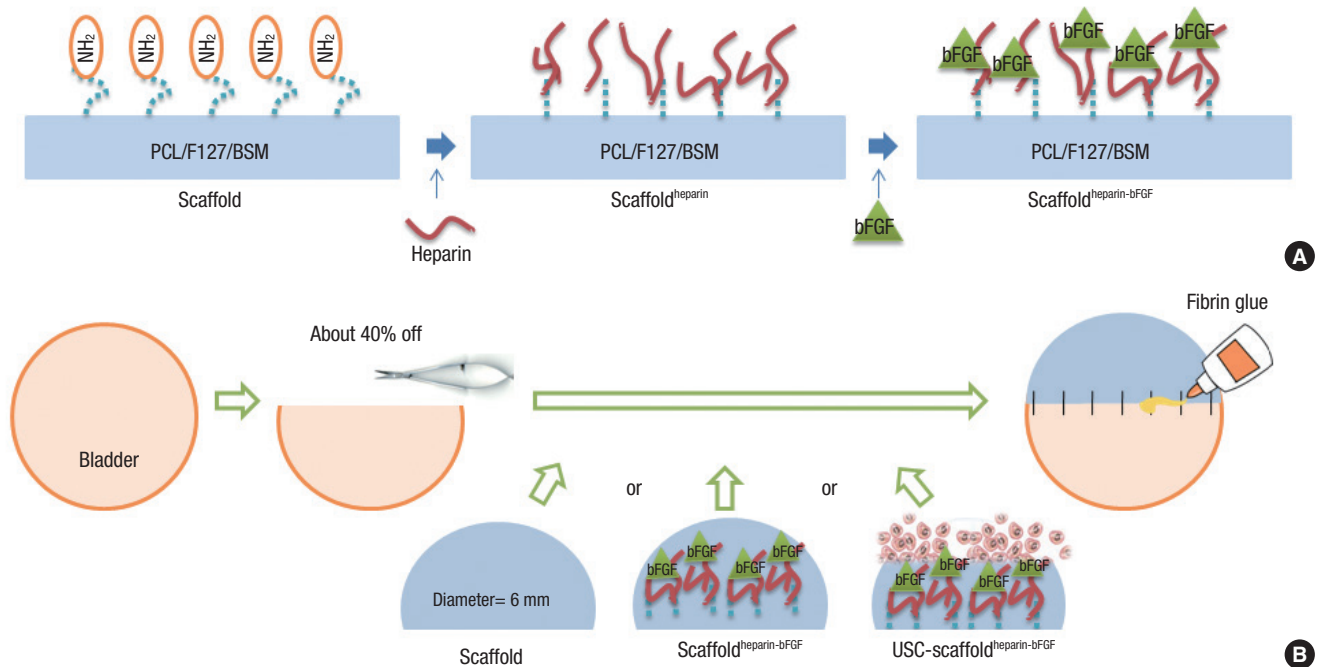


Fig. 1. Schematic diagram of the scaffold fabrication and operation procedures. (A) Procedures for fabrication of the heparin-immobilized bFGF-loaded scaffolds (Scaffold^{heparin-bFGF}) consisting of Polycaprolactone/Pluronic F127/bladder submucosa matrix (PCL/F127/BSM). (B) Bladder reconstruction operation procedure using the various scaffolds.

placed with fresh medium. The amount of bFGF was determined using a Quantikine Immunoassay kit, according to the manufacturer's instructions (Human bFGF Quantikine ELISA kit, R&D Systems, Minneapolis, MN, USA). An unmodified heparin scaffold was used as a control ($n = 3$).

Scaffold^{heparin-bFGF} surface morphology, biocompatibility, and effects on cell differentiation

Urine samples from the upper urinary tract were obtained from a 52-yr-old female patient. A volume of 100 mL of each urine sample was centrifuged, and the cell pellets were washed with PBS. The cells were cultured in mixed medium consisting of keratinocyte serum-free medium and progenitor cell medium (Gibco-Invitrogen, Grand Island, NY, USA) in a 1:1 ratio (21).

The surface morphology of the scaffolds and adherent cells on the scaffolds were assessed using a field emission scanning electron microscope (FE-SEM, S-4300, Hitachi, Hitachi-shi, Japan). The USC-loaded scaffolds were fixed in a 4% paraformaldehyde (PFA, Sigma-Aldrich) solution at 30°C for 45 min, followed by washing with dH₂O, drying, and coating with gold. The specimens were examined by FE-SEM at an acceleration voltage of 10 kV.

To analyze the cell adherence efficiency for the scaffold^{heparin-bFGF}, USCs (1×10^4 cells) were seeded on the scaffold (6 mm diameter, 0.4 mm thickness) and incubated overnight at 37°C and 50 rpm. After one day, the scaffolds were treated with DNA lysis buffer consisting of 0.1% sodium dodecyl sulfate (SDS, v/v), 1 mM ethylenediaminetetraacetic acid (EDTA), and 100 mM Tris-

HCl (pH 7.4). The unmodified scaffold (not loaded with bFGF) was used as a control. Samples were frozen and thawed repeatedly, and then incubated overnight. Total DNA in the samples was measured using a fluorescent DNA quantitation kit (Bio-Rad, Richmond, VA, USA), according to the manufacturer's instructions. DNA concentration measurements were confirmed using confocal microscopy (Axio Observer. Z1, Carl Zeiss).

To measure cell viability and proliferation, 5×10^3 cells were seeded on the scaffolds (10 mm diameter, 0.4 mm thickness), and a CCK-8 assay (Dojindo, Tokyo, Japan) was performed, according to the manufacturer's instructions. The unmodified scaffold was used as a control. For myogenic differentiation, USCs were seeded on the scaffold^{heparin-bFGF} in Dulbecco's modified Eagle medium (DMEM) containing non-essential amino acids, glutamine, and 15% fetal bovine serum (FBS, Gibco-Invitrogen). At approximately 95% confluence, $3 \mu\text{M}$ 5-aza-2'-deoxycytidine (Sigma-Aldrich) and 5 ng/mL of transforming growth factor β (TGF- β , Peprotech) were added to the culture medium for 24 hr and the cells were cultured up to 14 days. For urothelial cell differentiation, USCs were cultured with supernatant medium collected from human bladder urothelial cell cultures (Lonza, Walkersville, MD, USA) and cultured for 14 days.

Flow cytometric evaluation of cells (passage 3) was performed for mesenchymal stem cell markers (CD44, CD90, and CD105), smooth muscle cell markers (α -SM actin, Capponin I), and urothelium markers (pan-CK, CK19) (BD Biosciences, San Jose, CA, USA), according to the manufacturer's instructions. For real-time PCR, total RNA was extracted with an RNeasy kit (Qia-

Table 1. Primer sequences

Markers	Symbol	Full name	Sequences	
Stem cell marker	OCT4	Octamer-binding transcription factor 4	5'-TCAGCCAAACGACCATCTGC 5'-GCTTGATCGCTGCCCTTCT	
	SSEA4	Stage specific embryonic antigen 4	5'-TCCCAGGTTCAAGCGATTCTC 5'-CCAACATGGTGAACGCAGTC	
	NANOG	Nanog	5'-GCATCCGACTGTAAGAATCTTCA 5'-CATCTCAGCAGAAGACATTTGCA	
	ALP	Alkaline phosphatase	5'-ACGAGCTGAACAGGAACACGT 5'-CACCAGCAAGAAGAAGCCTTTG	
	C-KIT	c-kit	5'-GGCATCATGATCAAAAGTGTGAA 5'-CCCTCCTGGTCCACAGAACA	
Smooth muscle cell differentiation marker	PAX7	Paired box 7	5'-GCAAAATTGCTGCTCGTCA 5'-TGAAAACCTGGTCCATCTGCCT	
	MYOD	Myoblast determination protein	5'-ACAGCGCGGTTTTTCCAC 5'-AACCTAGCCCTCAAGGTTCCAG	
	DESMIN	Desmin	5'-GGAGAGGAGAGCCGGATCA 5'-GGGCTGGTTTCTCGGAAGTT	
	MYOSIN	Myosin	5'-AGGCGGAGAGGTTTTCCAA 5'-CTTGTAGTCCAAGTTGCCAGTCA	
	α -SM ACTIN	Alpha smooth muscle actin	5'-CAAGTGATCACCATCGGAAATG 5'-GACTCCATCCCATGAAGGA	
Epithelial cell differentiation marker	UP1a	Uroplakin 1A	5'-CGCTGGTGCCTGGATTG 5'-GGCACCCACACAAAAC	
	UP1b	Uroplakin 1B	5'-CAATTGCTGTGGCGTAAATGG 5'-ATAACACAGCATTGACGAGGCC	
	UP2	Uroplakin 2	5'-TCGTGCCAGGAACCAATTC 5'-GGATTCCATGTTCCCTCGAGG	
	CK7	Cytokeratin-7	5'-GGAACCTCATGAGCGTGAAGCT 5'-CCAGTGAATTCATCACAGAGATAT	
	CK13	Cytokeratin-13	5'-GGATGCTGAGGAATGGTTCCA 5'-GCTCTGTCTTGCTCCGTGATCT	
	CK18	Cytokeratin-18	5'-ATTGAGGAGAGCACACAGTGG 5'-TCTCATGGAGTCCAGGTCGATC	
	CK19	Cytokeratin-19	5'-CAGGTGAGTGTGGAGGTGGAT 5'-TCGCATGTCACTCAGGATCTTG	
	PAN-CK	Pan-cytokeratin	5'-GCCTCCTTGGCAGAAACAGAA 5'-GCACTCGGTTTCAGCTCGAAT	
	Housekeeping gene	β -ACTIN	β -actin	5'-ATCGTCCACCGCAAATGCT 5'-AAGCCATGCCAATCTCATCTTG

gen, Hilden, Germany), according to the manufacturer's instructions. A total of 2 μ g of RNA was used for cDNA synthesis using cDNA Reverse Transcription kits (Applied Biosystems, Warrington, UK). The primers were designed with Primer Express Software (Applied Biosystems), and were listed in Table 1. To analyze the data, the $2^{-\Delta\Delta Ct}$ method of relative quantification was adapted to estimate the copy numbers.

Urodynamic study, histology, and immunohistochemistry of reconstructed bladders

Twenty-five rats were divided to 5 groups: 1) control group, sham operated; 2) partial cystectomy group, approximately 40% defect was created in the dome of the bladder wall; 3) scaffold group, the unmodified scaffold was attached after partial cystectomy; 4) scaffold^{heparin-bFGF} group, the heparin-immobilized bFGF-loaded scaffold was attached after partial cystectomy;

and 5) USC-scaffold^{heparin-bFGF} group, scaffold^{heparin-bFGF} combined with 1×10^4 USCs was attached after partial cystectomy. The single-layer scaffold (disk form, diameter 6 mm) was sutured as a patch onto the defect of the bladder with 7-0 Vicryl sutures. Omentum was loosely wrapped over the graft and fixed with fibrin glue (Greenplast, Greencross, Seoul, Korea) (Fig. 1B).

An urodynamic study (filling cystometry) was performed on 5 animals from each group, at 8 weeks post-operation. Two animals with bladder calculi (scaffold group; n = 1, scaffold^{heparin-bFGF}; n = 1) were excluded from the urodynamic data collection. The bladder was filled with PBS, and maximal capacity was defined as the volume of infusion that triggered the first leakage of urine. Compliance was defined as maximal capacity/(pressure which triggered the first leakage) - (baseline pressure). Then, the entire bladder was removed, fixed in formalin, and the cross-sectional area of bladders divided in half was measured using ImageJ (<http://imagej.net/>). The bladder samples were embedded in paraffin and cut into 5 μ m sections that were stained using hematoxylin and eosin (H&E) and for immunohistochemical (IHC) staining. The regenerated smooth muscle and urothelial cell layers were identified by α -SM actin and pan-cytokeratin antibodies (Sigma-Aldrich), immune reaction was analyzed with cytotoxic T cell marker (CD8), and seeded human USCs on the scaffold were detected with human nuclei-specific antibody (HuNu, BD Biosciences).

Statistical analysis

All experiments were performed at least in triplicate on separate days. A *t*-test and a one-way analysis of variance (ANOVA) of Tukey's test were used for statistical analysis. All values are expressed as the mean \pm SD. Results are representative of at least three experiments.

Ethics statement

The study protocol using the cells from human urine was reviewed and approved by the institutional review board of Kyungpook National University Hospital (IRB No. KNUH 2012-10-018). Informed consent was obtained from the patient regarding urine sampling and use of cells. All experimental procedures using rats were reviewed and approved by the institutional animal care and use committee of Yeungnam University College of Medicine (YUMC-AEC2013-003).

RESULTS

Characteristics of the heparin-immobilized scaffold

Fig. 1A illustrates the procedures followed to functionalize the scaffold surface with primary amine groups and the subsequent heparin immobilization, followed by bFGF loading. The carboxylic acids exposed on the surface were used to produce surface amine groups, and the heparin was immobilized to the

surface via covalent conjugation (22). A toluidine blue assay was used to determine the amount of immobilized heparin, which was shown to be $0.72 \pm 0.11 \mu\text{g}/6 \text{ mm}^2$ (Fig. 2A). The fabricated scaffold had different sized pores on the surface at front and rear side, small and large; the pore sizes were -100 and -200 μm , respectively, and the heparin distribution was homoge-

neous when visualized with FITC-conjugated heparin (Fig. 2B).

Affinity and release of loaded bFGF

The amount of bFGF loaded into the scaffold^{heparin-bFGF} at days 1, 3, 7, 14, 21, and 28 was 33.68 ± 0.29 , 32.80 ± 0.39 , 30.39 ± 0.33 , 27.31 ± 0.25 , 25.67 ± 0.24 , and $26.03 \pm 0.30 \text{ pg/mL}$, and for the

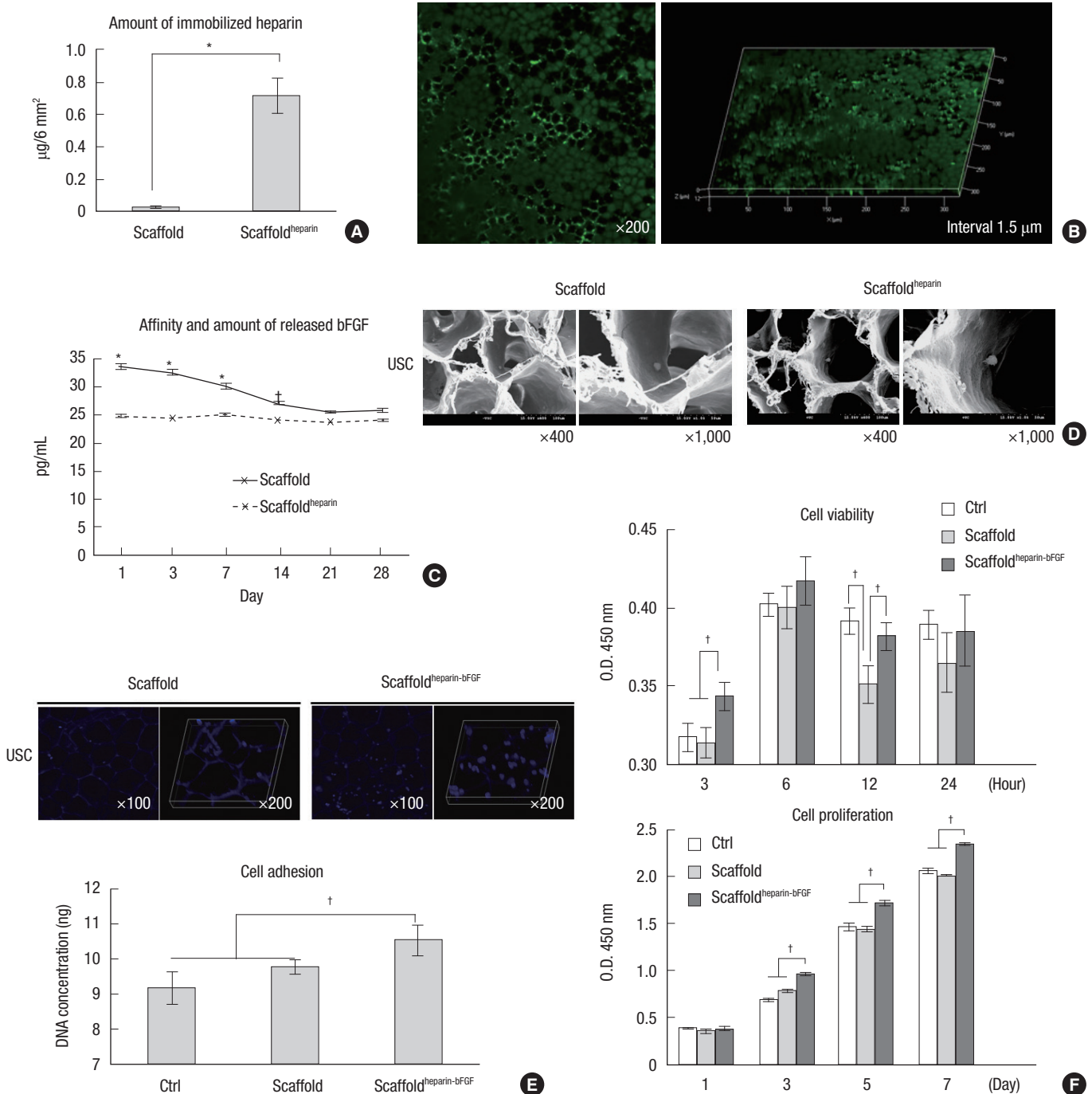


Fig. 2. Measurement of heparin, bFGF, and scaffold^{heparin-bFGF} biocompatibility. (A) Amount of immobilized heparin on the scaffold (n=3). (B) Visualization of immobilized heparin on the scaffold. (C) Affinity and amount of bFGF released from the heparin-immobilized scaffold for 28 days. An unmodified heparin scaffold was used as a control. (D) Field emission scanning electron microscope images of scaffold morphology and cells attached to the scaffold. (E) Cell adhesion to the scaffolds was determined by measuring the DNA concentration with Hoechst 33258 staining in confocal images. (F) Biocompatibility analysis of the scaffolds. Ctrl, culture plate dish; scaffold, unmodified scaffold; scaffold^{heparin-bFGF}, heparin-immobilized bFGF-loaded scaffold; USCs, urine derived stem cells; O.D., optical density. All data are presented as mean \pm SD (* $P < 0.01$; † $P < 0.05$).

Markers expression (%)	Mesenchymal stem cell			Smooth muscle		Urothelium	
	CD44	CD90	CD105	α -SM actin	Caponin I	pan-CK	CK19
Day 0	81.19	64.94	26.54	31.83	31.82	42.34	28.12
Day 14	51.03	42.22	9.50	96.71	70.13	77.87	76.66

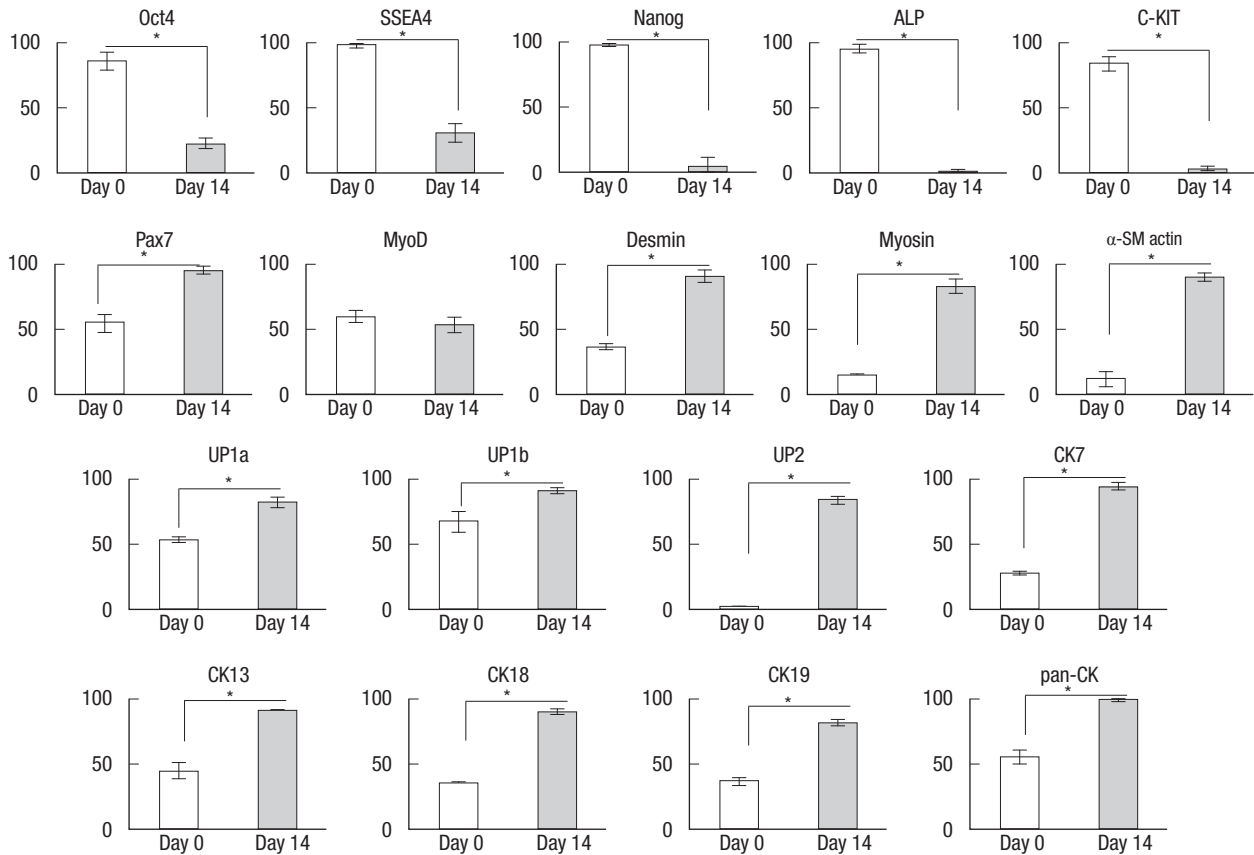
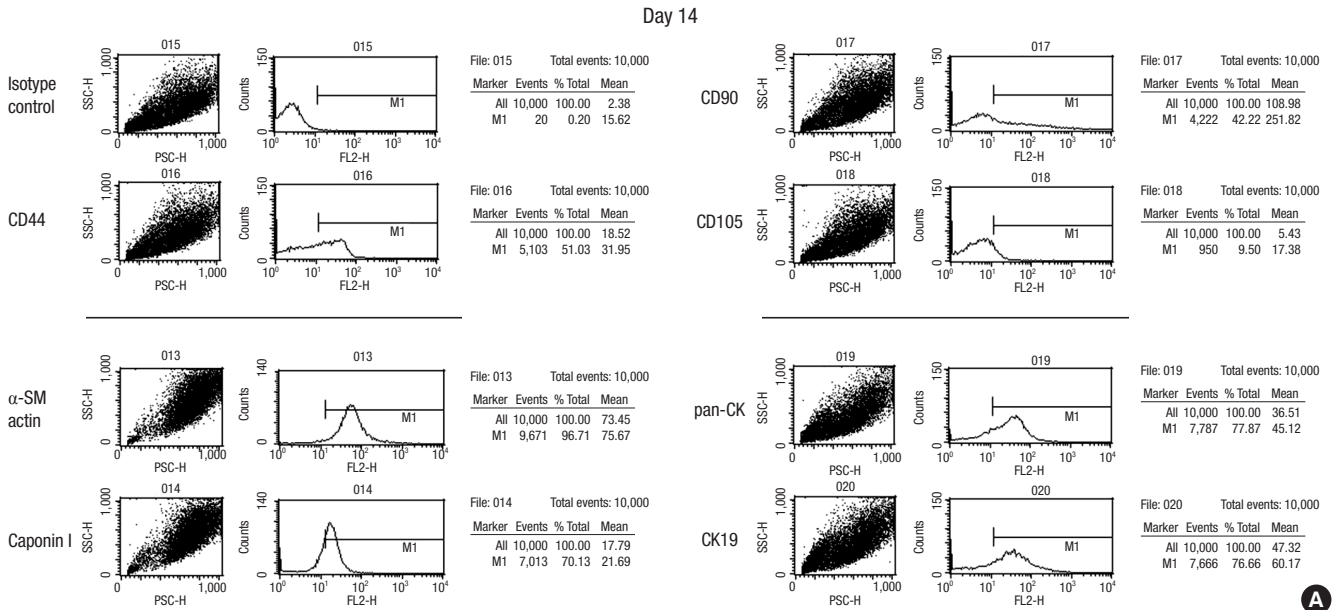


Fig. 3. Cell differentiation supported by the scaffold^{heparin-bFGF}. (A) USC differentiation (%) into smooth muscle and urothelial cells on the scaffold^{heparin-bFGF} and representative FACS images. (B) Real-time PCR analysis of stem cell, myogenic, and urothelial lineage markers at days 0 and 14. **P* < 0.01.

heparin unmodified scaffold was 25.02 ± 0.29 , 24.49 ± 0.07 , 25.14 ± 0.40 , 24.19 ± 0.23 , 23.89 ± 0.12 , and 24.19 ± 0.30 pg/mL, respectively (Fig. 2C). The initial concentration of bFGF on the heparin-immobilized scaffold revealed a high affinity and time-dependent release compared to the unmodified scaffold, and from day 21, the bFGF concentration became a basal level around 25.0 pg/mL. The unmodified scaffold showed rare affinity for bFGF, which means that heparin acts an effective linker to load of bFGF on the scaffold.

Scaffold^{heparin-bFGF} morphology and biocompatibility

The scaffolds exhibited a well-fabricated fibrous and porous structure, with large surface area (Fig. 2D). The pores had an average diameter of 50.8 ± 8.4 μ m. Analysis of cell adhesion based on DNA concentration showed that adhesion to the scaffold^{heparin-bFGF} was significantly higher than to the other surfaces (Fig. 2E). After culturing the cells for periods of 3, 6, 12, and 24 hr and 1, 3, 5, and 7 days, the viability and proliferation of USCs showed more viable cells present on the scaffold^{heparin-bFGF} (Fig. 2F); from day 3 of the culture, the absorbance value was significantly higher for the scaffold^{heparin-bFGF} than that of the other surfaces.

Differentiation into smooth muscle and urothelial cells on the scaffold^{heparin-bFGF}

When USCs were cultured on the scaffold^{heparin-bFGF} with smooth muscle and urothelium induction media, the cells were shown to express smooth muscle and urothelium surface markers at day 14 (Fig. 3A). The number of α -SM actin, Caponin I, pan-CK, and CK19-positive cells increased by 3.04, 2.20, 1.84, and 2.73 times, respectively, while, mesenchymal stem cell markers for CD44, CD90, and CD105 decreased by 0.63, 0.65, and 0.36 times, respectively.

The FACS results were confirmed with gene analysis through real-time PCR (Fig. 3B). At day 14 of differentiation, the cells exhibited significantly reduced expression of stem cell markers Oct4, SSEA4, Nanog, ALP, and c-Kit, while, markers indicative of smooth muscle cell (Pax7, MyoD, Desmin, Myosin, and α -SM actin) and urothelium cell (UP1a, UP1b, UP2, Ck7, Ck13, Ck18, Ck19, and pan-CK) differentiation were significantly increased.

Urodynamic study, histology, and immunohistochemistry

All rats for the in vivo study survived until the scheduled time of sacrifice, and there was no significant change in body weight or anastomosis problems observed during the experiment. The maximal bladder capacity and compliance at 8 weeks post operation was 2.60 ± 0.23 mL and 56.14 ± 9.00 μ L/cm H₂O for the control group, 1.46 ± 0.18 mL and 34.27 ± 4.42 μ L/cm H₂O for the partial cystectomy group, 1.76 ± 0.22 mL and 35.62 ± 6.69 μ L/cm H₂O for the scaffold group, 1.92 ± 0.29 mL and 40.74 ± 7.88 μ L/cm H₂O for the scaffold^{heparin-bFGF} group, and 2.34 ± 0.25 mL and 55.09 ± 11.81 μ L/cm H₂O for the USC-scaffold^{heparin-bFGF}

group (Table 2).

There was no diverticulum on the implanted portions for any group, which were covered on the outer surface by connective tissue, and 2 animals (scaffold group; n = 1, scaffold^{heparin-bFGF} group; n = 1) were observed to have bladder calculi formation. Gross image analysis showed that the USC-scaffold combination resulted in a reconstructed bladder with better shape and volume. The mean cross-sectional area of the reconstructed bladders were 16.85 ± 1.21 , 7.87 ± 1.37 , 9.67 ± 0.87 , 11.19 ± 0.87 , and 15.71 ± 1.34 mm² for the control, partial cystectomy, scaffold, scaffold^{heparin-bFGF}, and USC-scaffold^{heparin-bFGF} groups, respectively (Table 2) (Fig. 4A).

H&E and IHC analysis (Fig. 4B) showed that the USC-scaffold^{heparin-bFGF} group exhibited pronounced, well-differentiated, and organized smooth muscle bundle formation, while other groups exhibited thin muscle layer regeneration consisting of fibroblasts and connective tissue. With regard to the urothelium, a multi-layered and pan-cytokeratin-positive urothelium was observed at the reconstructed area for most of the groups, except for the scaffold group. The condensation of submucosal area was notably high in the USC-scaffold^{heparin-bFGF}. The scaffold group showed enhanced CD8 lymphocyte accumulation, while the USC-scaffold^{heparin-bFGF} showed scant accumulation of CD8-positive cells. The seeded human USCs were not detected at the USC-scaffold^{heparin-bFGF} group at week 8.

DISCUSSION

Current research suggests that the use of biomaterial based scaffolds seeded with autologous urothelial and smooth muscle cells is the best option for bladder tissue engineering (23). But, biomaterial based scaffolds lead to a number of complications, and autologous cells are often difficult to obtain. Therefore, we investigated the synergistic effect of a combination of USCs and heparin-immobilized bFGF-loaded scaffolds. This approach would provide development of novel composite biomaterial based scaffold and cell source.

Previously, we fabricated a scaffold containing BSM that we reported to have amine groups on the surface (12), and heparin was covalently immobilized to the exposed amine groups on the scaffold surface. Heparin is a highly sulfated glycosaminoglycan, which has binding affinity and activity maintaining of various growth factors (24). Because of these specific interactions with growth factors, heparin has been widely used in fabrication of bioactive matrices for growth factor delivery (25,26), and thus, we attempted bFGF-loading of our scaffold via heparin-immobilization. Comparison of a scaffold without surface modification to a heparin-immobilized scaffold showed higher bFGF loading for the modified scaffold, which was attributed to the ionic interactions that occurred between the positively charged bFGF protein (at physiological pH) and negatively

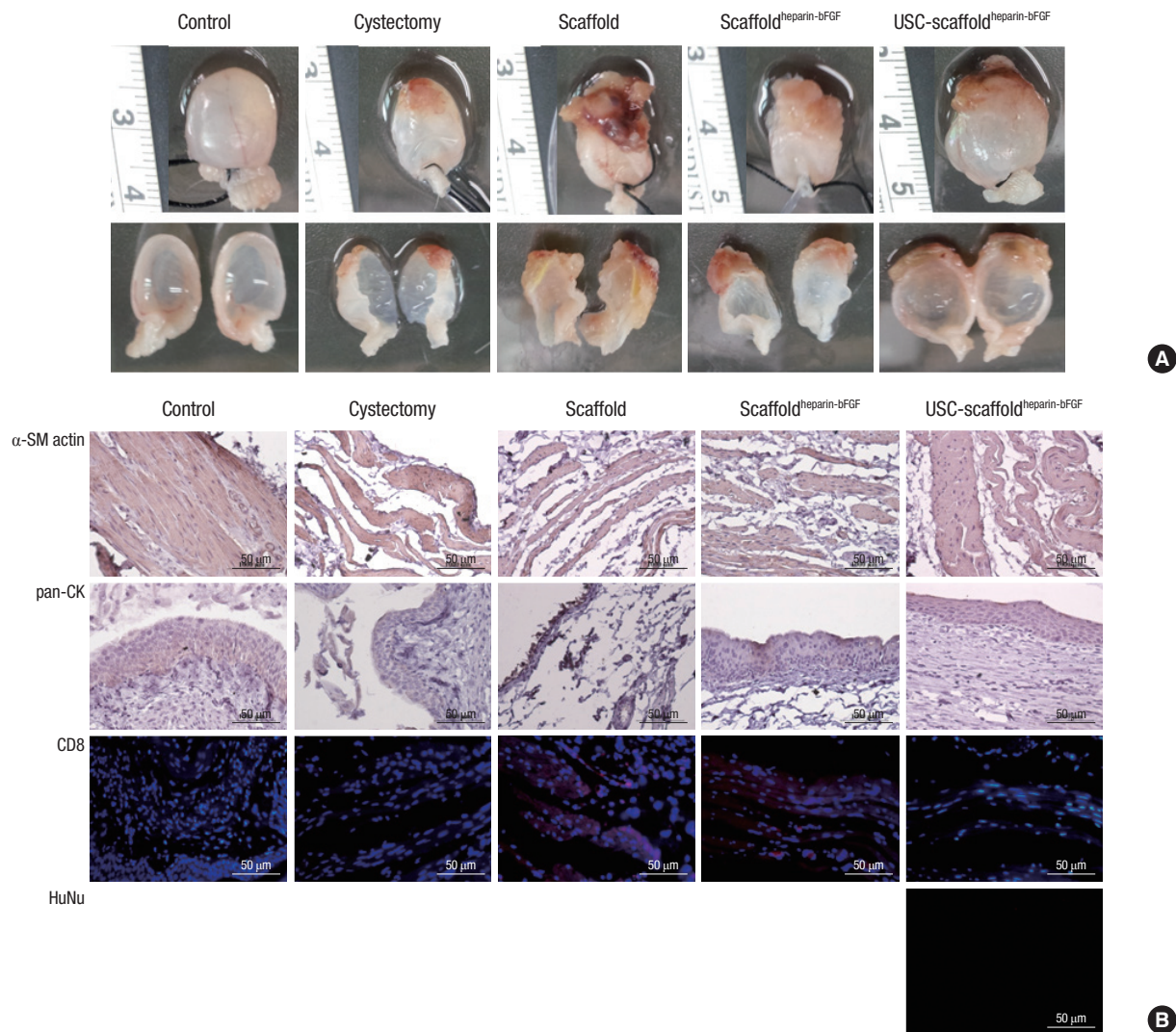


Fig. 4. Morphological and immunohistochemical (IHC) analysis. **(A)** Morphological analysis of retrieved bladder. **(B)** Analysis of α -SM actin, pan-CK, CD8, and HuNu expression with IHC. α -SM actin, α -smooth muscle actin; pan-CK, pan-cytokeratin; CD8, cluster of differentiation 8; HuNu, Human nuclei-specific antibody. Control, sham operated; partial cystectomy, approximately 40% defect was created in the dome of the bladder wall; scaffold, unmodified scaffold was attached after partial cystectomy; scaffold^{heparin-bFGF}, the heparin-immobilized bFGF-loaded scaffold was attached after partial cystectomy; USC-scaffold^{heparin-bFGF}, scaffold^{heparin-bFGF} combined with USCs was attached after partial cystectomy. Scale bar = 50 μ m. Magnification, 400 \times .

Table 2. Measurement of cross-sectional area and urodynamic results, including maximal bladder capacity and compliance

Parameters	Control	Partial cystectomy	Scaffold	Scaffold ^{heparin-bFGF}	USC-scaffold ^{heparin-bFGF}
Cross-sectional area, mm ² (mean \pm SD)	16.85 \pm 1.21	7.87 \pm 1.37	9.67 \pm 0.87	11.19 \pm 0.87	15.71 \pm 1.34
Maximal bladder capacity, mL (mean \pm SD)	2.60 \pm 0.23	1.46 \pm 0.18	1.76 \pm 0.22	1.92 \pm 0.29	2.34 \pm 0.25
Compliance, μ L/cm H ₂ O (mean \pm SD)	56.14 \pm 9.00	34.27 \pm 4.42	35.62 \pm 6.69	40.74 \pm 7.88	55.09 \pm 11.81

charged heparin (27,28). The observed sustained release pattern for the scaffold^{heparin-bFGF} was also likely caused by specifically bound bFGF on the heparin-immobilized surface (14).

In addition to a biocompatible scaffold, an appropriate cell source is also an essential requirement for tissue regeneration. USCs may play an important role in experimental research for urological organ regeneration and other urological-based applications, as they represent an optimal source due to their capacity for differentiation to myogenic and urothelial lineages

(16). In the present study, the heparin-immobilized bFGF-loaded surface supported USC behavior, including attachment, viability, proliferation, and differentiation. To analyze the effects of the scaffold^{heparin-bFGF} on cell viability and proliferation, USCs were cultured with the two different types of scaffolds. The proliferation of USCs cultured on the scaffold^{heparin-bFGF} was significantly higher than on the unmodified scaffold. In addition, the USC-scaffold^{heparin-bFGF} was shown to enhance myogenic and urothelial differentiation rates, indicating that the scaffold^{heparin-}

bFGF provides a suitable microenvironment for cell culture because bFGF promotes mesenchymal cell proliferation (29) and induces extracellular matrix production (13), which may improve the local microenvironment for supporting implanted cell proliferation and differentiation.

For the in vivo bladder regeneration study, the USC-scaffold-heparin-bFGF, scaffold^{heparin-bFGF}, and unmodified scaffold were implanted into the partially cystectomized bladders of rats to evaluate their potential for bladder tissue reconstruction. The images of the bladder specimens after dissection showed that the implanted scaffolds were attached in the bladder and covered with fibrous tissue. For the unmodified scaffold, the thick fibrous mass remained, and no expansion of the bladder volume was observed. The USC-scaffold^{heparin-bFGF} exhibited a thin fibrous mass and expanded bladder volume, which are indicative of bladder reconstruction. The scaffold^{heparin-bFGF} (without cells) yielded only a moderate result. The observed fibrous mass can also be used as an indicator of the inflammation caused by the scaffold, as previously described in a study reporting that fibrous tissue showed infiltration of neutrophils and macrophages (30). IHC analysis with the CD8 antibody showed that the unmodified scaffold exhibited an enhanced positive signal when compared to the other groups, indicating that the unmodified scaffold causes chronic inflammation, and surface modification and USCs could reduce this pathologic phenomenon.

The implanted scaffolds were not visible in the tissue sections because they were dissolved during the specimen-processing step using xylene. The histological features of the implanted grafts showed that the regenerated portions of the bladders in the USC-scaffold^{heparin-bFGF} group exhibited pronounced smooth muscle bundles, a multi-layered urothelium, condensed submucosa layer formation, and restored bladder volume. These anatomical reconstructions are essential for functional compliance. Other scaffold groups, however, showed only weak smooth muscle cell bundles, a thin urothelium, and loose submucosa regeneration at the graft. These results suggest that the seeded USCs contributed to the tissue regeneration. While the seeded cells were expected to survive for 2 weeks in vivo (31), we observed that the exogenous cells introduced in vivo were effective for bladder regeneration in comparison to the cells recruited from surrounding host tissues or circulating blood flow. The USC regenerative mechanism was not specifically identified in this paper, however, based on previous reports, it is presumed to result from the paracrine effects of tropic factors secreted from the USCs (31). Thus, the transplanted stem cells influenced the surrounding host cells, resulting in improved cell migration and differentiation into target cells.

In conclusion, the heparin-immobilized bFGF-loaded scaffold exhibits enhanced biocompatibility, and USCs seeded on

the scaffold^{heparin-bFGF} induces a synergistic effect, as indicated by increased bladder capacity, compliance, and histological tissue reconstruction signified by smooth muscle, urothelium, submucosa layer regeneration, and reduced inflammation, in a partial cystectomy rat model. Therefore, we propose that USC-scaffold^{heparin-bFGF} would be an ideal strategy for bladder reconstruction.

DISCLOSURE

The authors have no potential conflicts of interest to disclose.

AUTHOR CONTRIBUTION

Conceived and designed the experiments: Lee JN, Chun SY. Performed the experiments: Lee HJ, Jang YJ, Kim DH. Scaffold manufacturing: Oh SH, Lee JH. Analyzed the data: Song PH. Drafting of the manuscript: Chun SY, Lee JN. Critical revision of the manuscript for important intellectual content: Kwon TG. Statistical analysis: Lee JN. Obtaining funding: Kwon TG. Administrative, technical, or material support: Song PH, Kim DH. Approval of the final manuscript: Kwon TG.

ORCID

Jun Nyung Lee <http://orcid.org/0000-0002-6342-9846>
 So Young Chun <http://orcid.org/0000-0003-4500-4956>
 Hyo-Jung Lee <http://orcid.org/0000-0002-1179-0373>
 Yu-Jin Jang <http://orcid.org/0000-0001-5660-3001>
 Seock Hwan Choi <http://orcid.org/0000-0003-3796-2601>
 Dae Hwan Kim <http://orcid.org/0000-0002-2083-0154>
 Se Heang Oh <http://orcid.org/0000-0002-4635-6809>
 Phil Hyun Song <http://orcid.org/0000-0002-3801-258X>
 Jin Ho Lee <http://orcid.org/0000-0002-1528-3416>
 Tae Gyun Kwon <http://orcid.org/0000-0002-4390-0952>

REFERENCES

- Jednak R. *The evolution of bladder augmentation: from creating a reservoir to reconstituting an organ.* *Front Pediatr* 2014; 2: 10.
- Salem SA, Hwei NM, Bin Saim A, Ho CC, Sagap I, Singh R, Yusof MR, Md Zainuddin Z, Idrus RB. *Poly(lactic-co-glycolic acid) mesh coated with fibrin or collagen and biological adhesive substance as a prefabricated, degradable, biocompatible, and functional scaffold for regeneration of the urinary bladder wall.* *J Biomed Mater Res A* 2013; 101: 2237-47.
- Kim BS, Mooney DJ. *Engineering smooth muscle tissue with a pre-defined structure.* *J Biomed Mater Res* 1998; 41: 322-32.
- Chen W, Shi C, Yi S, Chen B, Zhang W, Fang Z, Wei Z, Jiang S, Sun X, Hou X, et al. *Bladder regeneration by collagen scaffolds with collagen binding human basic fibroblast growth factor.* *J Urol* 2010; 183: 2432-9.
- Lanza RP, Langer RS, Vacanti JP. *Principles of tissue engineering.* Amsterdam: Academic Press, 2013.

6. Geng HQ, Tang DX, Chen F, Wu XR, Zhou X. *The bladder submucosa acellular matrix as a cell deliverer in tissue engineering*. *World J Pediatr* 2006; 2: 57-60.
7. Zhang Y, Kropp BP, Lin HK, Cowan R, Cheng EY. *Bladder regeneration with cell-seeded small intestinal submucosa*. *Tissue Eng* 2004; 10: 181-7.
8. Zambon JP, de Sá Barretto LS, Nakamura AN, Duailibi S, Leite K, Magalhaes RS, Orlando G, Ross CL, Peloso A, Almeida FG. *Histological changes induced by Polyglycolic-Acid (PGA) scaffolds seeded with autologous adipose or muscle-derived stem cells when implanted on rabbit bladder*. *Organogenesis* 2014; 10: 278-88.
9. Gomelsky A, Dmochowski RR. *Tissue Engineering for Neurogenic Bladder*. In: Wein AJ, Andersson KE, Drake MJ, Dmochowski RR, editors. *Bladder dysfunction in the adult : the basis for clinical management*. New York, NY: Springer, 2014, p265-76.
10. Roth CC, Mondalek FG, Kibar Y, Ashley RA, Bell CH, Califano JA, Madhally SV, Frimberger D, Lin HK, Kropp BP. *Bladder regeneration in a canine model using hyaluronic acid-poly(lactic-co-glycolic-acid) nanoparticle modified porcine small intestinal submucosa*. *BJU Int* 2011; 108: 148-55.
11. Yu DS, Lee CF, Chen HI, Chang SY. *Bladder wall grafting in rats using salt-modified and collagen-coated polycaprolactone scaffolds: preliminary report*. *Int J Urol* 2007; 14: 939-44.
12. Jang YJ, Chun SY, Kim GN, Kim JR, Oh SH, Lee JH, Kim BS, Song PH, Yoo ES, Kwon TG. *Characterization of a novel composite scaffold consisting of acellular bladder submucosa matrix, polycaprolactone and Pluronic F127 as a substance for bladder reconstruction*. *Acta Biomater* 2014; 10: 3117-25.
13. Lee M, Wu BM, Stelzner M, Reichardt HM, Dunn JC. *Intestinal smooth muscle cell maintenance by basic fibroblast growth factor*. *Tissue Eng Part A* 2008; 14: 1395-402.
14. Yoon JJ, Chung HJ, Lee HJ, Park TG. *Heparin-immobilized biodegradable scaffolds for local and sustained release of angiogenic growth factor*. *J Biomed Mater Res A* 2006; 79: 934-42.
15. Pigott JH, Ishihara A, Wellman ML, Russell DS, Bertone AL. *Investigation of the immune response to autologous, allogeneic, and xenogeneic mesenchymal stem cells after intra-articular injection in horses*. *Vet Immunol Immunopathol* 2013; 156: 99-106.
16. Chun SY, Kim HT, Lee JS, Kim MJ, Kim BS, Kim BW, Kwon TG. *Characterization of urine-derived cells from upper urinary tract in patients with bladder cancer*. *Urology* 2012; 79: 1186.e1-7.
17. Oh SH, Kim JR, Kwon GB, Namgung U, Song KS, Lee JH. *Effect of surface pore structure of nerve guide conduit on peripheral nerve regeneration*. *Tissue Eng Part C Methods* 2013; 19: 233-43.
18. Jonnalagadda SB, Gollapalli NR. *Kinetics of reduction of toluidine blue with sulfite-kinetic salt effect in elucidation of mechanism*. *J Chem Educ* 2000; 77: 506.
19. Lee AC, Yu VM, Lowe JB 3rd, Brenner MJ, Hunter DA, Mackinnon SE, Sakiyama-Elbert SE. *Controlled release of nerve growth factor enhances sciatic nerve regeneration*. *Exp Neurol* 2003; 184: 295-303.
20. Smith PK, Mallia AK, Hermanson GT. *Colorimetric method for the assay of heparin content in immobilized heparin preparations*. *Anal Biochem* 1980; 109: 466-73.
21. Zhang Y, McNeill E, Tian H, Soker S, Andersson KE, Yoo JJ, Atala A. *Urine derived cells are a potential source for urological tissue reconstruction*. *J Urol* 2008; 180: 2226-33.
22. Jeon O, Kang SW, Lim HW, Chung JH, Kim BS. *Long-term and zero-order release of basic fibroblast growth factor from heparin-conjugated poly(L-lactide-co-glycolide) nanospheres and fibrin gel*. *Biomaterials* 2006; 27: 1598-607.
23. Atala A. *Tissue engineering of human bladder*. *Br Med Bull* 2011; 97: 81-104.
24. Sasisekharan R, Ernst S, Venkataraman G. *On the regulation of fibroblast growth factor activity by heparin-like glycosaminoglycans*. *Angiogenesis* 1997; 1: 45-54.
25. Wang XH, Li DP, Wang WJ, Feng QL, Cui FZ, Xu YX, Song XH. *Covalent immobilization of chitosan and heparin on PLGA surface*. *Int J Biol Macromol* 2003; 33: 95-100.
26. Steffens GC, Yao C, Prével P, Markowicz M, Schenck P, Noah EM, Pal-lua N. *Modulation of angiogenic potential of collagen matrices by covalent incorporation of heparin and loading with vascular endothelial growth factor*. *Tissue Eng* 2004; 10: 1502-9.
27. Cai S, Liu Y, Shu XZ, Prestwich GD. *Injectable glycosaminoglycan hydrogels for controlled release of human basic fibroblast growth factor*. *Biomaterials* 2005; 26: 6054-67.
28. Liu LS, Ng CK, Thompson AY, Poser JW, Spiro RC. *Hyaluronate-heparin conjugate gels for the delivery of basic fibroblast growth factor (FGF-2)*. *J Biomed Mater Res* 2002; 62: 128-35.
29. Kanematsu A, Yamamoto S, Noguchi T, Ozeki M, Tabata Y, Ogawa O. *Bladder regeneration by bladder acellular matrix combined with sustained release of exogenous growth factor*. *J Urol* 2003; 170: 1633-8.
30. Lech M, Gröbmayer R, Weidenbusch M, Anders HJ. *Tissues use resident dendritic cells and macrophages to maintain homeostasis and to regain homeostasis upon tissue injury: the immunoregulatory role of changing tissue environments*. *Mediators Inflamm* 2012; 2012: 951390.
31. Kim BS, Chun SY, Lee JK, Lim HJ, Bae JS, Chung HY, Atala A, Soker S, Yoo JJ, Kwon TG. *Human amniotic fluid stem cell injection therapy for urethral sphincter regeneration in an animal model*. *BMC Med* 2012; 10: 94.